Biochimica et Biophysica Acta 1840 (2014) 485–494

Contents lists available at ScienceDirect

Biochimica et Biophysica Acta

journal homepage: www.elsevier.com/locate/bbagen

Differential response of DU145 and PC3 prostate cancer cells to ionizing radiation: Role of reactive oxygen species, GSH and Nrf2 in radiosensitivity

Sundarraj Jayakumar [a], Amit Kunwar [b], Santosh K. Sandur [a,*], Badri N. Pandey [a], Ramesh C. Chaubey [a,1]

[a] Radiation Biology and Health Sciences Division, Bhabha Atomic Research Centre, Mumbai 400 085, India
[b] Radiation and Photochemistry Division, Bhabha Atomic Research Centre, Mumbai 400 085, India

ARTICLE INFO

Article history:
Received 10 May 2013
Received in revised form 14 September 2013
Accepted 1 October 2013
Available online 9 October 2013

Keywords:
Ionizing radiation
Radiosensitivity
Prostate cancer
Nrf2
PC3
DU145

ABSTRACT

Background: Radioresistance is the major impediment in radiotherapy of many cancers including prostate cancer, necessitating the need to understand the factors contributing to radioresistance in tumor cells. In the present study, the role of cellular redox and redox sensitive transcription factor, Nrf2 in the radiosensitivity of prostate cancer cell lines PC3 and DU145, has been investigated.
Materials and methods: Differential radiosensitivity of PC3 and DU145 cells was assessed using clonogenic assay, flow cytometry, and comet assay. Their redox status was measured using DCFDA and DHR probes. Expression of Nrf2 and its dependent genes was measured by EMSA and real time PCR. Knockdown studies were done using shRNA transfection.
Results: PC3 and DU145 cells differed significantly in their radiosensitivity as observed by clonogenic survival, apoptosis and neutral comet assays. Both basal and inducible levels of ROS were higher in PC3 cells than that of DU145 cells. DU145 cells showed higher level of basal GSH content and GSH/GSSG ratio than that of PC3 cells. Further, significant increase in both basal and induced levels of Nrf2 and its dependent genes was observed in DU145 cells. Knock-down experiments and pharmacological intervention studies revealed the involvement of Nrf2 in differential radio-resistance of these cells.
Conclusion: Cellular redox status and Nrf2 levels play a causal role in radio-resistance of prostate cancer cells.
General significance: The pivotal role Nrf2 has been shown in the radioresistance of tumor cells and this study will further help in exploiting this factor in radiosensitization of other tumor cell types.

1. Introduction

Radiotherapy is one of the major treatment modalities for cancers. More than 60% of the cancers are treated by radiation therapy either alone or in combination with chemotherapy or surgery. But the therapeutic efficacy of radiotherapy is hindered by the difference in the intrinsic radiosensitivity of different tumor cells. Therefore, it is very important to understand about the radiosensitivity, its molecular determinants, and outcome of such studies would be useful in prediction and modulation of radiosensitivity [1].

Radiation kills the tumor cells by producing reactive oxygen species (ROS) like hydroxyl radical, hydrogen peroxide, and superoxide which cause damage to biomolecules including DNA (indirect effect) or by directly causing DNA damage (direct effect). The proportion of direct and indirect damage depends on the quality and type of radiation. Gamma radiation kills cancer cells mainly by indirect damage. Intracellular antioxidants like glutathione, thioredoxin reductase, glutathione peroxidase, catalase, superoxide dismutase, etc. form the first line of defense against ROS induced oxidative stress in the cells [2,3]. These antioxidants help cells in scavenging ROS and salvaging biomolecules from oxidative damage.

Prior studies have established that the intracellular levels of most of the above enzymatic and non-enzymatic anti-oxidants are regulated by a redox sensitive transcription factor nuclear factor-E2-related factor 2 (Nrf2) [4,5]. Under normal conditions, Nrf2 protein is bound to an inhibitor protein Kelch-like-ECH-associated protein (Keap1). This binding of Keap1 protein to Nrf2 leads to ubiquitination and degradation of Nrf2 by proteasomal pathway [6]. Under oxidative stress conditions, critical cysteine residues present on the Keap1 protein get oxidised and thereby disrupting the binding of Keap1 to Nrf2. Then Nrf2 undergoes a rapid translocation into the nucleus, binds to antioxidant response elements (ARE), which are present in the promoter regions of its target antioxidant genes such as heme oxygenase 1 (HO1), NADH quinone oxidoreductase 1 (NQO1), the glutamate cysteine ligase catalytic subunit (GCLC), and thioredoxin reductase 1 (TXRD1), and facilitates their transcription [6]. Therefore, Nrf2 and its dependent genes may play a crucial

* Corresponding author at: Radiation Biology & Health Sciences Division, Bhabha Atomic Research Centre, Mumbai 400085, India. Tel.: +91 22 25595356; fax: +91 22 25505151.
E-mail address: sskumar@barc.gov.in (S.K. Sandur).
[1] Present address: C-11-6, Kendriya Vihar, Kharghar, Navi Mumbai, India.

0304-4165/$ – see front matter © 2013 Elsevier B.V. All rights reserved.
http://dx.doi.org/10.1016/j.bbagen.2013.10.006

role in determining radiosensitivity of tumor cells. Indeed few recent studies carried out in non-small-cell lung cancer [7] and esophageal squamous cancer cells [8] reporting the involvement of Nrf2 in radioresistance of tumor cells support the above hypothesis. However, such studies need to be performed under different scenarios and in different cell types in order to exploit Nrf2 as one of the targets for improving the effectiveness of radiotherapy.

Prostate cancer is one of the most commonly diagnosed non-cutaneous malignancies in men. Surgical removal, hormone ablation therapy and radiotherapy are the major treatment modalities for the prostate cancer. Radiotherapy can be used as curative treatment of clinically localized prostate cancer [9]. However, the radiation resistance has become a practical impediment to the radiotherapy of prostate cancers. Despite the significant advances in treatment modalities, prostate cancer is one of the leading causes of death due to cancer in men. Especially the treatment of androgen independent prostate cancers has become a challenging aspect. The tumors which are androgen independent also invariably show chemoresistance and radioresistance [10,11]. Therefore understanding the molecular mechanisms and the factors which determine the radioresistance of this tumor type is very important and would be helpful in improving the therapeutic efficacy of the radiotherapy of prostate cancer. Many studies have dwelled into this aspect of radioresistance of prostate cancer cells and have demonstrated the role aurora kinase B [11], P21 activated kinase-6 [12] and 12-lipoxygenase [13] in radioresistance of prostate cancer cells. Furthermore, Zhang et al. [6] observed point mutations in Keap1 protein of prostate cancer cells and found transcriptional and post-transcriptional regulation of Keap1 protein which affects the treatment response in prostate tumor cells. But the role of Nrf2 and its dependent genes in radiation resistance of androgen independent prostate cancer is not reported. This may help in exploiting Nrf2 as a target in improving therapeutic efficacy. Among the various prostate tumor cells, PC3 and DU145 cells which lack androgen receptors are useful as many prostate cancer patients show androgen independent tumor growth [11].

In the present study, we investigated the role of Nrf2 and its dependent genes in determining radiosensitivity of prostate cancer cells using two well-characterised androgen independent cell lines viz., PC3 and DU145 which are known to exhibit differences in their chemotherapeutic response.

2. Materials and methods

2.1. Chemicals

Dulbecco's modified Eagles medium (DMEM), antibiotics (streptomycin and penicillin), sodium bicarbonate, crystal violet, Tris–HCl, ethylenediaminetetraacetic acid (EDTA), sodium chloride (NaCl), dimethyl sulfoxide (DMSO), dihydrodichloroflourescin diacetate (H_2-DCFDA), dihydorhodamine 123 (DHR 123), propidium iodide (PI), sodium citrate, triton X-100, ribonuclease A, all-trans retinoic acid (ATRA), tin protoporphyrin (SnPP), glutathione (reduced and oxidized) and diethyl pyrocarbonate (DEPC) were purchased from Sigma-Aldrich (MO, USA). Fetal bovine serum (FBS) and trypsin-EDTA were from Himedia (Mumbai, India). Lipofectamine was purchased from Invitrogen (Bangalore, India) and short hairpin RNA (shRNA) plasmids were purchased from OriGene (MD, USA).

2.2. Cell lines and irradiation

PC3 and DU145 cells were obtained from the National Institute for Research in Reproductive Health, Mumbai. Cells were maintained as exponentially growing monolayer in DMEM supplemented with 10% FBS, penicillin and streptomycin in humidified incubator maintained at 37 °C with 5% CO_2 in air.

Cells were irradiated (dose rate: 2.5 Gy/min) using ^{60}Co gamma cell 220 irradiator (AECL, Canada). For comet assay, exponentially growing cells were harvested by trypsinization. Cells obtained were thus suspended in complete medium followed by irradiation at 4 °C. After irradiation, samples to be processed immediately (0 min) were kept in ice, whereas, for repair kinetic studies, samples were incubated at 37 °C for various time intervals (15, 30, 60, and 120 min). For RNA isolation, exponentially growing cells (2×10^6 cells) were seeded overnight in culture dish (BD Falcon, USA), irradiated (either 4 or 8 Gy) and cultured for 24 h before RNA isolation. For electrophoretic mobility shift assay (EMSA), exponentially growing cells were seeded overnight, irradiated and incubated for 24 h before performing EMSA.

2.3. Clonogenic assay

Clonogenic assay was performed as mentioned previously [14]. Exponentially growing cells were seeded on 60 mm dishes and allowed to adhere overnight in culture conditions. These cultures were exposed to various doses of γ-radiation (1, 2, 4, 6, 8 and 10 Gy). For studies involving the inhibition of Nrf2 and HO1 activities, cells were treated with the respective inhibitors (10 μM ATRA or 15 μM SnPP respectively) for 1 h before irradiation. After irradiation dishes were kept in the incubator for 15 days for the colony development. After the colony development dishes were washed with PBS, fixed with methanol and then stained using 0.5% crystal violet followed by rinsing the dishes with tap water. Colonies were counted using a stereo microscope. A colony was considered when there were at least 50 or more cells. Survival fraction was calculated using following formula:

$$\text{Survival fraction} = \text{No.of colonies}/[\text{no.of cells plated X}(\text{plating efficiency}/100)].$$

2.4. Apoptosis assay by PI staining

For apoptosis assay, cells were plated for overnight followed by radiation exposure. Forty eight hours after radiation exposure, cells were harvested, fixed with 70% ethanol and stained using propidium iodide (PI) staining solution (0.5 μg/ml PI, 10 μg/ml ribonuclease A, 0.1% sodium citrate and 0.1% Triton X-100). A total of 20,000 cells were acquired using the Partec flow cytometer and were analyzed using FlowJo software.

2.5. Homogenous caspase assay

Homogenous caspase assay was performed using homogenous caspase assay kit (Roche, Germany). With this assay the combined activities of caspase 3 and caspase 7 were measured. This assay is based on the fluorescence emanated due to the cleavage of the pro-fluorescent substrate attached to a peptide, by caspase 3 or caspase7. Exponentially growing cells were plated and allowed to adhere for overnight followed by radiation exposure. At 48 h after radiation exposure, cells were harvested and 40,000 cells were incubated along with the incubation buffer containing substrate peptide attached to Rhodamine 110. One hour after the incubation, Rhodamine 110 fluorescence was measured using a flourimeter (λ_{ex} — 485 nm, λ_{em} — 521 nm) and relative caspase activity was calculated in comparison to control cells.

2.6. Comet assay

To determine the magnitude of DNA damage, neutral comet assay was performed as mentioned previously [15]. Briefly, control and irradiated cells were suspended in 0.8% low melting agarose and were layered on to frosted slides pre-coated with 1% normal agarose. After solidification, slides were kept in the lysis buffer at 4 °C for 60 min. For equilibration, the slides were transferred to electrophoretic tank containing 0.5× Tris–Borate–EDTA buffer. Slides were electrophoresed in the same buffer for 30 min at 0.8 V/cm. After electrophoresis, slides were neutralised (0.4 M

Table 1
Primer sequences of different genes whose expression has been checked by quantitative real time RT-PCR.

Genes	Forward primer	Reverse primer
β-Actin	CTGGAACGGTGAAGGTGACA	AAGGGACTTCCTGTAACAATGCA
Nrf2	AGCATGCCCTCACCTGCTACTTTA	ACTGAGTGTTCTGGTGATGCCACA
HO1	AGAGGGAATTCTCTTGGCTGGCTT	ATGCCATAGGCTCCTTCCTCCTTT
GCLC	ATGGAAGTGGATGTGGACACCAGA	AACTCCCTCATCCATCTGGCAACT
TXRD1	TCCTATGTCGCTTTGGAGTGC	GGACCTAACCATAACAGTGACGC
Keap1	CTGCAGGATCATACCAAGCAGG	GAACATGGCCTTGAAGACAGG

Tris–HCl), stained (1× SYBR Green I dye) and visualised at 40× magnifications using fluorescence microscope (Axioplan, Carl-Zeiss, Germany). For every treatment, two slides were prepared and at least 50 images were grabbed per slide. The images were analyzed using CASP software (www.casplab.com) to obtain % DNA in tail, which is considered as the reliable parameter for representing the DNA damage in comet assay.

2.7. Electrophoretic mobility shift assay

In order to assay the DNA binding ability of Nrf2 in PC3 and DU145 cells, electrophoretic mobility assay (EMSA) was carried out as mentioned previously [16]. Briefly, at 24 h after irradiation, nuclear extract was prepared from the nuclear pellet by repeated vortexing. Protein was quantified from the nuclear extracts, and equal amount of protein was incubated with the ^{32}P labeled Nrf2 binding consensus sequence (5′-TGG GGA ACC TGT GCT GAG TCA CTG GAG-3′, Santa Cruz Biotechnology, CA, USA) for 1 h and then it was loaded onto 7.6% polyacrylamide gel and electrophoresed at 70 mA. After the electrophoresis, gel was vacuum dried and the signal was developed using phosphor imager.

2.8. Quantitative real time RT-PCR

To quantify the mRNA expression of genes, quantitative real time reverse transcriptase polymerase chain reaction (RT q-PCR) was used [17]. Total RNA was isolated using TRI reagent (Sigma, MO, USA) as

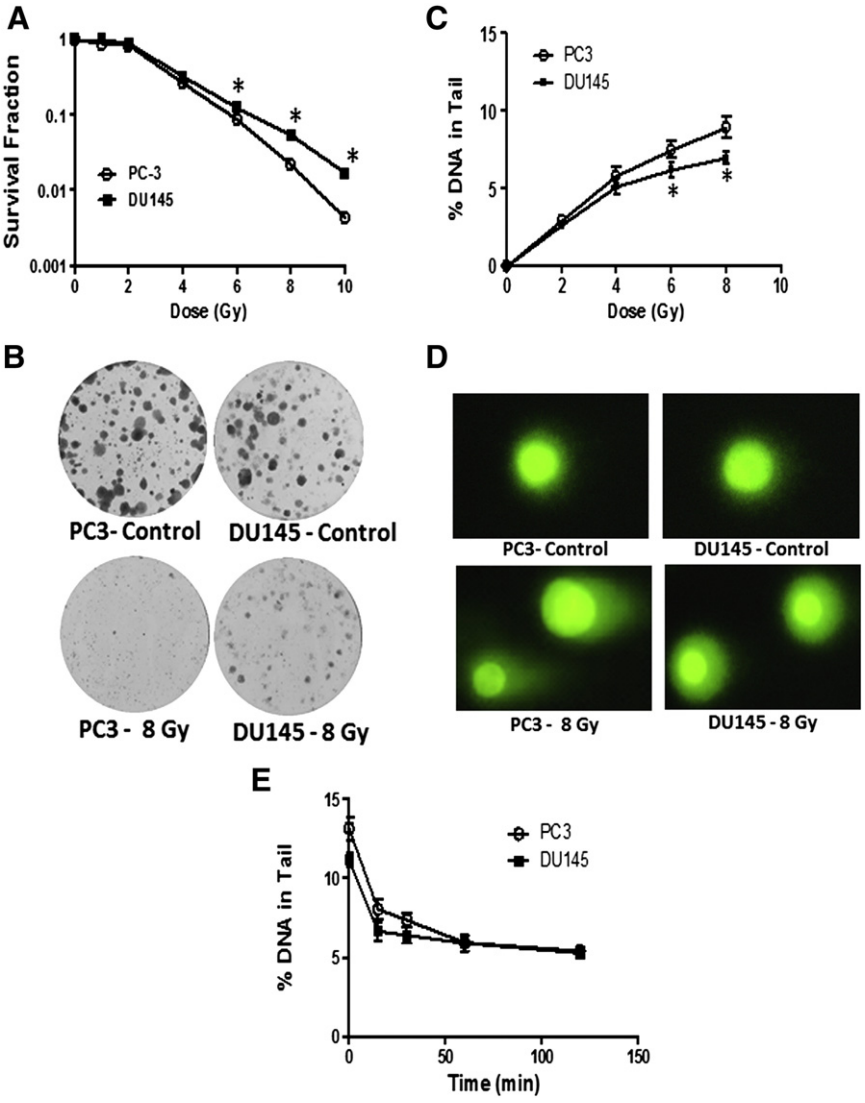

Fig. 1. Radiosensitivity profile of PC3 and DU145 cells, as determined by clonogenic assay (A and B), DNA damage (C and D) and DNA repair kinetics (E) obtained by neutral comet assay. For clonogenic assay, exponentially growing cells have been irradiated, grown for two weeks, stained and the number of colonies was counted and the survival fraction has been plotted. Three independent experiments were performed in triplicates each time and mean ± SEM has been plotted. Representative image of clonogenic assay of PC3 and DU145 cells after 8 Gy radiation exposure has been shown (B). Neutral comet assay was performed in the control as well as irradiated cells at different time points after irradiation as described in the Materials and methods section. From the neutral comet assay, at least 50 cells per slide were microscopically grabbed and analyzed for DNA damage. Two slides were prepared for every treatment, and the mean ± SEM of three independent experiments was plotted. Representative images of PC3 and DU145 cells obtained after exposure to 8 Gy of radiation has been shown (D). *$P < 0.05$ in comparison to respective PC3 group.

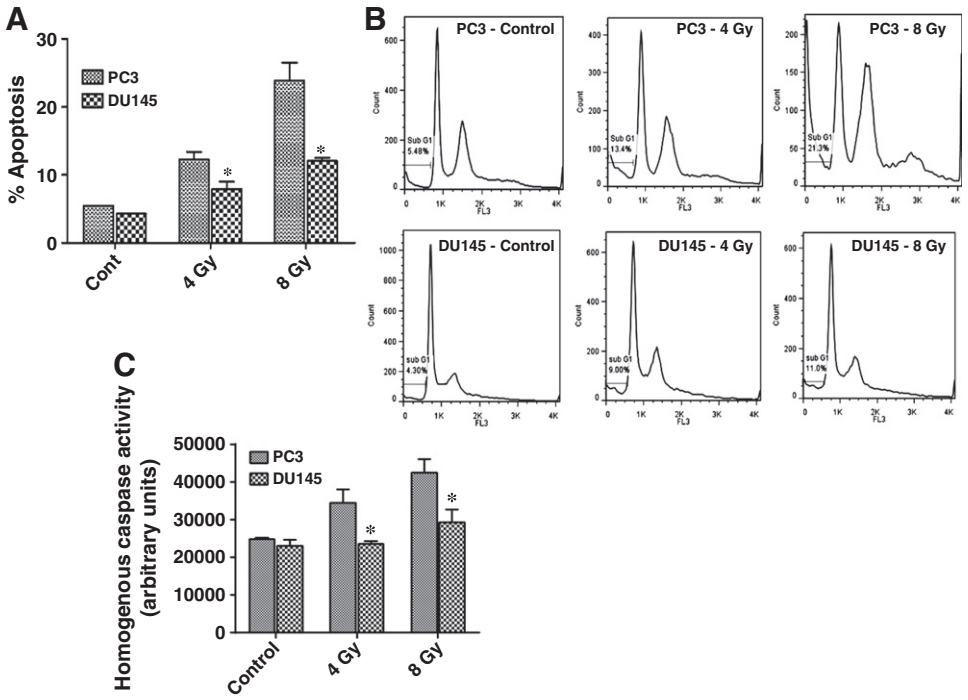

Fig. 2. Radiation response of PC3 and DU145 cells, as determined by apoptosis enumerated by PI staining (A and B), and homogenous caspase assay (C). For PI assay, cells were plated for overnight followed by radiation exposure. Forty eight hours after radiation exposure, cells were harvested, fixed and stained using PI staining solution. A total of 20,000 cells were acquired using the Partec flow cytometer and were analyzed using FlowJo software. Percentages of cells in pre-G1 peak were represented as cells undergoing apoptosis. Mean ± SEM obtained from two independent experiments done in triplicates, has been plotted. For homogenous caspase assay, cells were harvested at 48 h after the radiation exposure and processed accordingly using homogenous caspase assay kit. Arbitrary units of mean fluorescence obtained in two experiments done in triplicates have been plotted with SEM. *$P < 0.05$ in comparison to respective PC3 group.

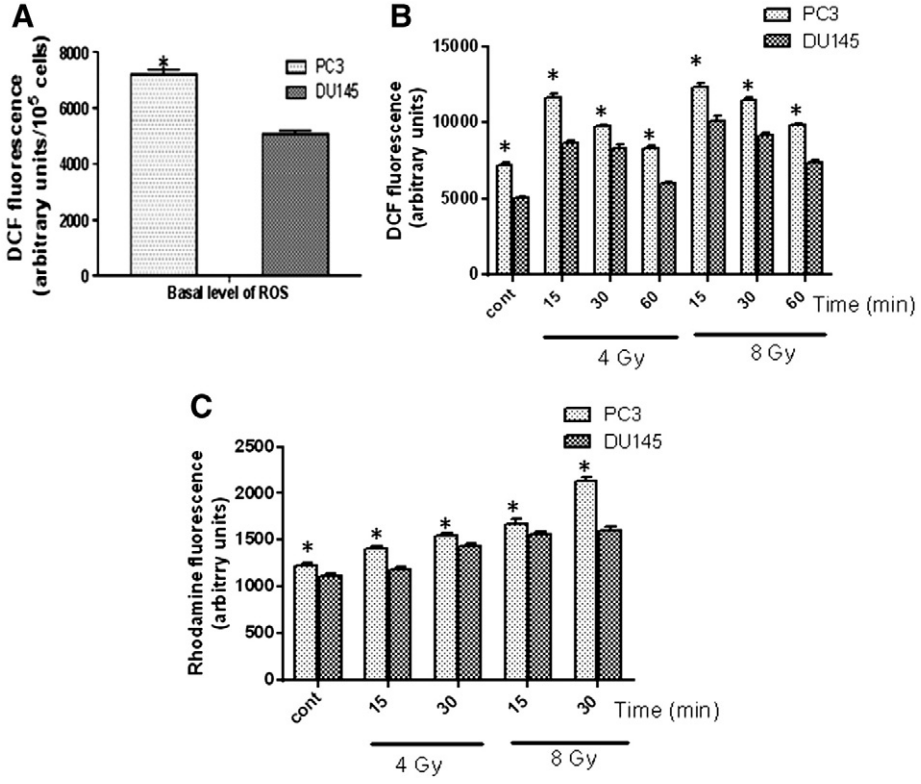

Fig. 3. Levels of reactive oxygen species as measured by DCF fluorescence in PC3 and DU145 cells in control (A), after 4 Gy and 8 Gy (B). Mitochondrial ROS as estimated by rhodamine in PC3 and DU145 cells after radiation exposure of 4 Gy and 8 Gy (C). For measuring ROS, either DCFDA or DHR was added to cells 30 min prior to irradiation, fluorescence of DCF or rhodamine recorded at different time intervals and the mean ± SEM was plotted. Three independent experiments in triplicates at each time point were performed. *$P < 0.05$ in comparison to respective DU145 group.

per manufacturer's instructions. Two micrograms of total RNA was used for the synthesis of cDNA by reverse transcription (cDNA synthesis kit, Sigma, MO, USA). PCR reactions were set up by mixing 10× SYBR green PCR mix with 5 μl of 2 times diluted cDNA templates, 1 μl each of forward and reverse primers (0.5 μM; Table 1), and 3 μl of PCR-grade water in 20 μl reaction mixture. The above reaction mixtures were amplified in the following steps: step 1—denaturation at 95 °C for 5 min; step 2—denaturation at 95 °C for 15 s; step 3—annealing at 57 °C for 15 s; step 4—extension at 72 °C for 20 s; and step 5—melting curve analysis. Steps 2–4 were repeated for 40 cycles using the Rotor Gene 3000 (Corbett Life Science, Australia). The threshold cycle values obtained from the above runs were used for calculating the fold change in gene expression by REST-384 version 2 software. The expressions of genes were normalized against that of a housekeeping gene, β-actin, and the relative change in the expression was plotted with respect to control group.

2.9. ROS measurement

For measuring intra-cellular cytosolic ROS levels, 1×10^5 cells were plated in 24 well plates for overnight. Then cells were treated with oxidation sensitive DCF-DA (a final concentration of 10 μM) in culture medium for 30 min at 37 °C prior to irradiation. After irradiation, the fluorescence of DCF in cells was measured (λ_{ex} — 485 nm, λ_{em} — 535 nm) at different time intervals [18]. Similarly for measuring mitochondrial ROS, dihydrorhodamine 123 at a final concentration of 10 μM was added to the cells, incubated for 30 min prior to irradiation and the rhodamine fluorescence was measured (λ_{ex} — 511 nm, λ_{em} — 536 nm) at various time intervals after irradiation [19].

2.10. Measurement of GSH and GSSG levels

Glutathione (GSH) and glutathione disulphide (GSSG) levels were measured as described previously [20]. Measurement of GSH by this method involves the oxidation of GSH by the sulfhydryl reagent 5,5′-dithio-bis(2-nitrobenzoic acid) (DTNB) to form the yellow derivative 5′-thio-2-nitrobenzoic acid (TNB), measurable at 412 nm. For measuring GSSG, the GSSG formed was recycled to GSH by glutathione reductase in the presence of NADPH and then measured by DTNB reduction method.

2.11. Measurement of thioredoxin reductase activity

Thioredoxin reductase 1 (TXRD1) activity was measured using a kit (Thioredoxin reductase assay kit, Cayman Chemical Company, USA) by following manufacturer's protocol. Briefly, DTNB reduction was measured in the absence and presence of aurothiomalate, a specific TXRD1 inhibitor that allows for the correction of TXRD1 independent DTNB reduction. By calculating the difference between the above two conditions, TXRD1 activity was estimated.

2.12. Knockdown of Nrf2 and HO-1 expression using short hairpin RNA (ShRNA)

Nrf2 and HO-1 expression was knocked down by transfecting cells with shRNA. For this purpose, exponentially growing cells were transfected with either NRF2 or random sequence shRNA, using lipofectamine-2000 as mentioned in the manufacturer's protocol (Invitrogen, Bangalore, India). Cells were harvested after 24 h of transfection and were plated for clonogenic survival assay. At 48 h after transfection, cells were exposed to various doses of irradiation and their clonogenic survival was seen after 15 days.

2.13. Statistical analysis

Statistical analysis was performed using GraphPad Prism 5.0 software (La Jolla, CA, USA). Student's *t*-test was used for comparing the means of two groups. One-way ANOVA was performed to test the significance when more than two groups were involved. Values were considered significantly different if $P < 0.05$.

3. Results

3.1. DU145 cells exhibits higher magnitude of radioresistance than PC3 cells

Clonogenic assay was used to evaluate the radiosensitivity of PC3 and DU145 prostate tumor cells. Cells were exposed to various doses of gamma radiation ranging from 1 to 10 Gy and their survival fraction was calculated after 15 days. Among the two cell lines DU145 cells showed more radioresistance than PC3 cells. Though the radiosensitivity of PC3 was comparable to that of DU145 at 0.5 and 2 Gy, PC3 cells showed a relative decrease in their survival fraction in comparison to DU145 cells as the dose of radiation increased (Fig. 1A and B). For example survival fractions estimated for PC3 cells at 2 and 10 Gy were 0.83 and 0.004 respectively, whereas that for DU145 0.89 and 0.02 respectively. The dose required to bring down the survival fraction from 0.1 to 0.01 for PC3 and DU145 cells was calculated to be 3 and 4.5 Gy respectively. Although both these tumor cells are from the same tissue of origin, a significant difference in their radiosensitivity was apparent in clonogenic survival assay. Differential radiation response of these two cells was also evaluated by DNA damage by neutral comet assay after exposing the cells to various doses of gamma radiation (2–8 Gy). The results revealed increased magnitude of DNA damage in PC3 cells in comparison to that of DU145 cells at all the doses with more significant differences at the higher doses (Fig. 1C and D). We also studied the DNA damage repair kinetics by assessing the extent of DNA damage at different time intervals (up to 2 h) after radiation exposure, by neutral comet assay. DU145 cells showed faster recovery of DNA damage in comparison to PC3 cells (Fig. 1E). In order to further evaluate the differential radiosensitivity of the above tumor cells, we have estimated the

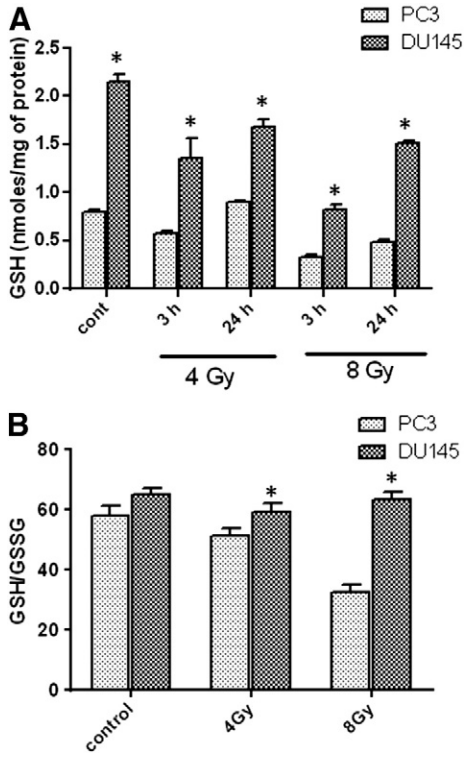

Fig. 4. Level of GSH and GGH/GSSG ratio in PC3 and DU145 cells. GSH levels were measured at 3 h and 24 h (A) after radiation exposure. GSH to GSSG ratio measured after 24 h (B) after radiation exposure. Three independent experiments were performed in triplicates at each time point and mean ± SEM has been plotted. *$P < 0.05$ in comparison to respective PC3 group.

cell death using propidium iodide staining followed by flow cytometry. For example, after 8 Gy of radiation exposure, 24% of PC3 cells underwent apoptosis (% cells in pre-G1 peak) as compared to 12% of DU145 cells (Fig. 2A and B). To confirm the results obtained by PI assay, caspase activity was also evaluated in these two cell lines after 4 Gy and 8 Gy radiation exposures. Homogenous caspase activity (activity of caspases 3 and 7) was observed to be significantly higher in PC3 cells in comparison to that of DU145 cells after 4 Gy and 8 Gy radiation exposures (Fig. 2C). Thus from clonogenic survival assay, apoptosis assay and DNA damage assay, it was clearly evident that among the two cell lines, DU145 cells showed more radioresistance than PC3 cells.

3.2. Intracellular redox environment of DU145 cells is more reducing than that of PC3 cells

Since PC3 and DU145 exhibited differences in radiosensitivity, we further investigated the redox state of these cells by estimating ROS and GSH levels under both the control and irradiated (4 and 8 Gy) conditions. Interestingly PC3 cells which were observed to be radiosensitive showed higher basal as well as induced level of cytosolic ROS (measured by DCF fluorescence) in comparison to that of DU145 cells (Fig. 3A and B). In both the tumor cell lines, maximum intracellular ROS was observed at 15 min following irradiation, which declined with progress of time. Unlike DCF, rhodamine fluorescence, which measures mitochondrial ROS showed time dependent increase following irradiation. As observed with DCF, the rhodamine fluorescence was lower in DU145 cells compared to that of PC3 cells at all the time points studied suggesting increased level of mitochondrial ROS in PC3 cells compared to that of DU145 cells (Fig. 3C).

In agreement with ROS levels, DU145 cells showed significantly higher basal GSH content than that of PC3 cells (Fig. 4A). On irradiation both the cells showed depletion in their GSH but with progress of time, DU145 cells showed much faster recovery of GSH content than that of PC cells (Fig. 4A). The ratio of GSH and GSSG was also significantly higher in DU145 cells than that of the PC3 cells and it was maintained even at 24 h after irradiation at different doses (Fig. 4B). Taken together these results suggest a reducing type of redox environment in DU145 cells compared to that of PC3 cells and this could be the reason for the enhanced tolerability of DU145 against radiation exposure.

3.3. DU145 cells exhibits elevated levels of Nrf2 and its dependent transcripts than PC3 cells after radiation exposure

Anticipating the involvement of redox sensitive transcription factor Nrf2 in the observed differences in redox environment of the above two cell lines, we measured the activation of Nrf2 in these cells under irradiated condition using EMSA. DU145 cells showed higher basal levels of Nrf2 in comparison to PC3 cells (Fig. 5A). Moreover, PC3 cells, which exhibited high radiosensitivity, showed significantly lower level of Nrf2 than DU145 cells after radiation exposure (4 and 8 Gy). We also measured the mRNA expression level of Nrf2 in these cells by RT q-PCR at

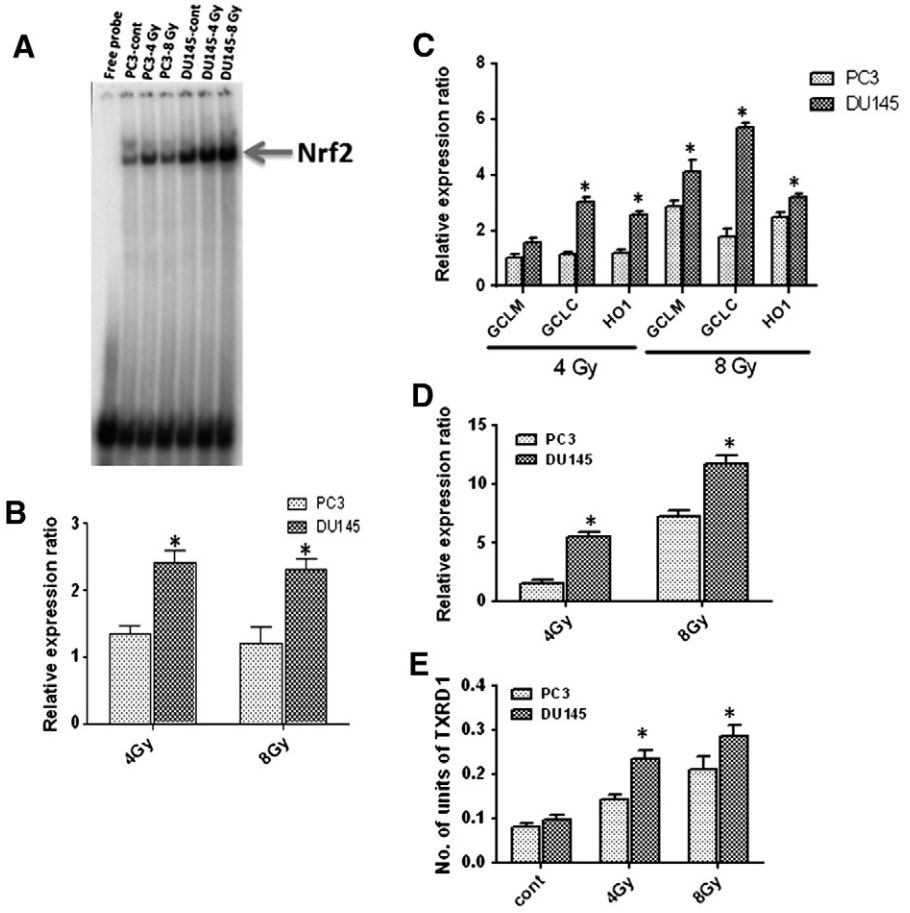

Fig. 5. Nuclear levels of Nrf2 as assessed by EMSA in nuclear extract (A), mRNA levels of Nrf2 (B) and its dependent genes GCLM, GCLC, HO1 (C) and TXRD1 (D) in PC3 and DU145 cells after 4 Gy and 8 Gy of radiation exposure. Biochemical activity of TXRD1 enzyme in PC3 and DU145 cells after exposure to 4 Gy and 8 Gy of radiation (E) was also estimated. For EMSA protein lysate was made from nuclear pellets, and equal amount of protein was incubated with the ^{32}P labeled Nrf2 binding consensus sequence and followed by electrophoresis. After the electrophoresis, gel was vacuum dried and the signal was developed using phosphor imager. Representative image of the three experiments has been shown. Gene expression was analyzed by real-time q-PCR, at 24 h after exposing the cells to 4 Gy/8 Gy of gamma irradiation. The bars represent the mean ± SEM obtained from two independent experiments done in triplicates. *$P < 0.05$ in comparison to respective PC3 group.

24 h after radiation exposure. DU145 cells showed two fold higher induction of Nrf2 levels in comparison to PC3 cells after 4 and 8 Gy of radiation exposure (Fig. 5B).

As there was a difference seen in Nrf2 levels between these two cell lines, we also evaluated the expression levels of Nrf2 dependent genes like HO1, GCLC and TXRD1 after exposing to either 4 Gy or 8 Gy. Following 4 Gy of radiation exposure, DU145 cells showed 5.69, 2.6 and 5.46 fold upregulation in the expression of GCLC, HO1 and TXRD1 genes over control respectively (Fig. 5C and D). However in PC3 cells, these genes did not show significant upregulation after radiation exposure. Biochemical activity of TXRD1 was also measured in the cell lysate at 24 h after radiation exposure, which indicated a significant increase in DU145 cells than in PC3 cells after 4 Gy radiation exposure (Fig. 5E).

Since Keap1 protein plays a key role in regulating the Nrf2 pathway, we have evaluated the mRNA levels of Keap1 in PC3 and DU145 cells. Basal levels of Keap1 gene in DU145 cells were found to be two fold lower than that of the PC3 cells (Fig. 6A). Further, the changes in mRNA levels of Keap1 were also examined after exposure to radiation and found that both PC3 and DU145 cells showed a negative regulation of Keap1 gene. The extent of this negative regulation was marginally higher in PC3 cells than that observed in DU145 cells. But the differences were not statistically significant (Fig. 6B).

3.4. Nrf2 and HO1 levels determine radiosensitivity in DU145 and PC3 cells

In order to confirm the role of Nrf2 and its dependent genes in radiosensitivity of tumor cells, we examined the survival fraction of PC3 and DU145 cells after radiation exposure, in the presence or absence of inhibitors of Nrf2 and HO1 namely ATRA and SnPP, respectively. The presence of these inhibitors significantly reduced the survival fraction of the above tumor cells against the radiation exposure. Treatment with the above inhibitors prior to radiation exposure at 4 Gy reduced the survival fraction of PC3 cells from 0.21 to 0.01 and that of DU145 cells from 0.31 to 0.03 (Fig. 7A and B). Similarly, in DU145 cells, SNPP and ATRA treatments decreased the survival fraction from 0.08 to 0.014 after 8 Gy radiation exposure, whereas the survival fraction of PC3 cells reduced from 0.015 to 0.007. Further, to corroborate this evidence of involvement of Nrf2 in radiosensitivity, we have employed knockdown approach by transfecting shRNA against Nrf2 into DU145 cells. A nonspecific shRNA having scrambled sequence was used as a control. The transfected cells were exposed to 4 Gy of radiation and their survival fraction was analyzed. The cells, which were transfected with shRNA targeting Nrf2 prior to radiation exposure, showed a drastic decrease in survival fraction (0.035), in comparison to the cells transfected with scrambled shRNA (0.28) after 4 Gy irradiation (Fig. 7C and D). It was also observed that the cells transfected with Nrf2 specific shRNA showed significant reduction in survival even without the radiation treatment. Clonogenic survival assay was also performed in DU145 cells after knocking down the expression of HO1 (an Nrf2 dependent gene). Though HO1 knockdown itself has not exhibited any significant reduction in survival, radiation exposure of HO1 knockdown cells exhibited significant reduction in survival fraction (Fig. 7E and F). These evidences suggested the involvement of redox regulated transcription factor in determining radiosensitivity of prostate tumor cells.

4. Discussion

Molecular mechanisms governing the radiosensitivity/radioresistance of tumor cells are not clearly understood and there is a need for further research in this area. In order to study the molecular players which determine radiosensitivity, we have chosen two prostate tumor cells namely, PC3 and DU145, which are androgen independent cells, known to have differential chemotherapeutic response [21,22]. However, differential radiosensitivity and underlying mechanism have not been investigated in these two prostate cancer cell lines. In this study, we have investigated the radiosensitivity of these two prostate cancer cells and made an attempt to rationalize molecular differences between them contributing to their differential radiosensitivity. These two cell lines showed difference in their radiosensitivity as measured by clonogenic survival fraction after irradiation (1–10 Gy) and PC3 cells were found to be more radiosensitive than DU145 cells. This difference was more prominent at higher doses (>8 Gy) than at the lower doses (<4 Gy) of radiation exposure (Fig. 1A). In apoptosis analysis PC3 cells also showed more sensitivity towards radiation than DU145 cells. Radiosensitive PC3 cells also showed more DNA damage than DU145 cells. Though these two tumor cells exhibited significant difference in DNA damage after the radiation exposure, following DNA repair kinetics, there was no significant difference in residual DNA damage between these two cells. These results are in corroboration with earlier observation that the initial DNA damage observed by neutral comet assay is a good marker of radiosensitivity than the residual DNA damage [15].

Since ROS is known to play an important role in the cytotoxic action of ionizing radiation, we have evaluated basal and inducible levels of ROS in these two tumor cells. PC3 cells, which are radiosensitive among the two cell lines, showed higher basal as well as inducible levels of ROS on radiation exposure (Fig. 3A–C). High levels of ROS accumulation can lead to increased DNA damage and a variety of other cellular responses including cell cycle arrest, senescence and apoptosis [23]. Similar to cytosolic ROS, mitochondrial ROS levels was also found to be more in radiosensitive PC3 cells after the radiation exposure. Cells employ many enzymatic and non-enzymatic antioxidants to counter the effect of ROS and to bring back cell homeostasis [24]. One of the most versatile protectors of such antioxidants is GSH. GSH protects cells from radiation damage by several mechanisms including radical scavenging, restoration of damaged molecules by hydrogen donation, reduction of peroxides and maintenance of protein thiols in the reduced state [25]. Therefore, we have evaluated the level of GSH, and GSH to GSSG ratio in both PC3 and DU145 tumor cells under control and irradiated conditions. A relatively radiosensitive PC3 cells showed low basal

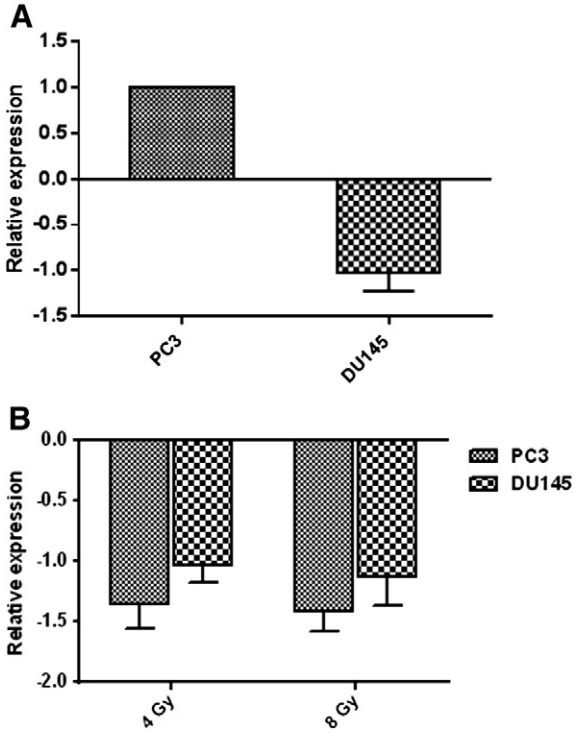

Fig. 6. mRNA levels of Keap1 in control (A) and after radiation exposure (B) in PC3 and DU145 cells. Gene expression was analyzed by real-time q-PCR, at 24 h after exposing the cells to 4 Gy/8 Gy of gamma irradiation. The error bars represent the mean ± SEM obtained from two independent experiments done in triplicates.

level of GSH and also showed faster depletion of GSH after radiation exposure (Fig. 4A and B). The radioresistant DU145 cells showed faster recovery from oxidative stress and this was also supported by their high GSH to GSSG ratio in comparison to that of PC3 cells. Increased accumulation of ROS combined with the faster depletion of GSH may be responsible for higher DNA damage observed in PC3 cells after radiation exposure. It has also been shown that thiol depletion can lead to higher radiation induced apoptosis [26].

Since we have observed differences in cellular redox environment between these two cell lines after irradiation, we hypothesised that the transcription factor which controls the enzymes involved in GSH synthesis may be playing key role in determining radiosensitivity. Nrf2 is the transcription factor which involved in the transcription of the enzymes involved in GSH biosynthesis [27,28]. Apart from the enzyme which is involved in GSH biosynthesis (GCLC and GCLM), glutathione peroxidase enzymes (GPX1, GPX2 and GPX3) and thioredoxin families (thioredoxin, TXRD1, peroxiredoxin) have also been shown to be the transcriptional targets of Nrf2 [7,29,30]. In the present study, we have observed that Nrf2 activation and its dependent genes were upregulated in DU145 cells in comparison to those in PC3 cells (Fig. 5A–E). Keap1 protein plays a major role in regulating the nuclear Nrf2 levels. Therefore we have evaluated the Keap1 mRNA levels in these two cell types and found that relative levels of Keap1 were lower in DU145 cells than that in PC3 cells. These reduced levels of Keap1 may be one of the reasons for higher basal levels of Nrf2 in DU145 cells. Reduced levels of Keap1 in DU145 cells may be attributed to the reported hyper-methylation in the Keap1 promoter of the DU145 cells [6]. GCLC, an enzyme which is involved in biosynthesis of GSH, has shown significant upregulation in radioresistant DU145 cells in comparison to that of PC3 cells. This could have played a role in restoring the thiol balance in these cells quickly contributing to their radioresistance as compared to PC3 cells. Moreover, when we inhibited the Nrf2 by inhibitors as well as shRNA we observed a drastic reduction in survival fraction of radioresistant DU145 cells after the radiation exposure. It was also observed that the cells transfected with Nrf2 specific shRNA showed significant reduction in survival even without the

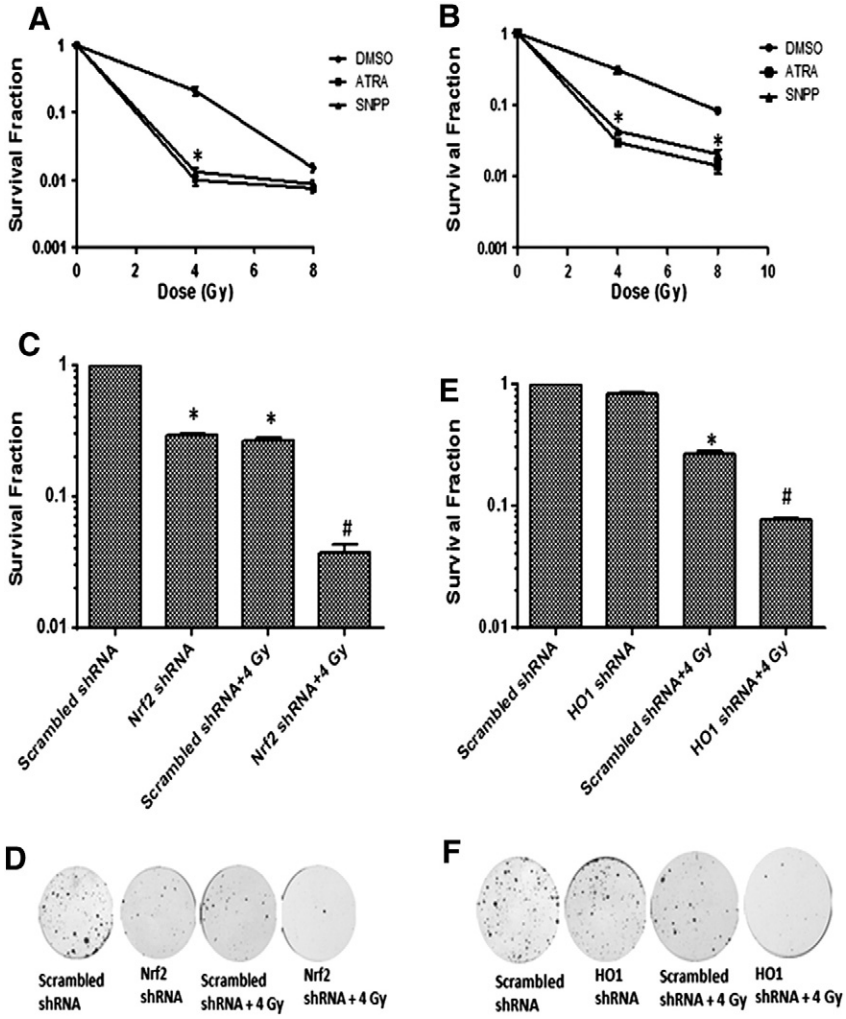

Fig. 7. Survival fraction of PC3 (A) and DU145 (B) cells after exposure to radiation in the presence of ATRA (Nrf2 inhibitor) or SnPP (HO1 inhibitor). Exponentially growing cells were plated, treated with inhibitors, irradiated and followed by clonogenic assay. Three independent experiments were performed in triplicates each time and mean ± SEM has been plotted. $^{*}P < 0.05$ in comparison to DMSO control group. Survival fraction was also calculated in DU145 cells after knocking down the expression of Nrf2 expression (C) or HO1 expression (D) which is exposed to radiation, 48 h after transfection with shRNA targeting Nrf2 or HO1 expression. Survival fraction was assessed by clonogenic assay by counting the colonies developed at 15 days after treatment and radiation exposure. A nonspecific shRNA containing scrambled sequences was used as control. Two independent experiments were performed with triplicates each time. Mean ± SEM has been plotted. Representative clonogenic dishes belonging to various treatment groups have also been shown (E and F). $^{*}P < 0.05$ in comparison to scrambled shRNA group. $\#P < 0.05$ in comparison to scrambled shRNA + 4 Gy group.

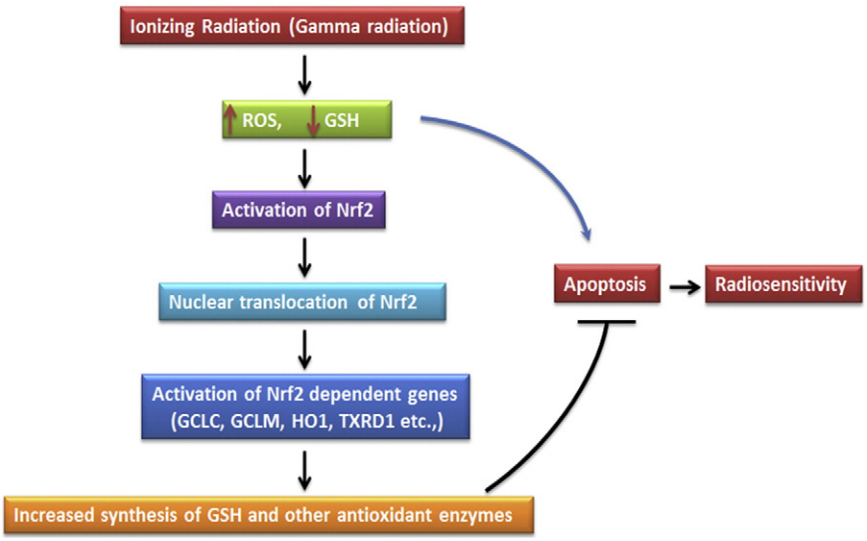

Fig. 8. Schematic diagram representing the role of ROS, GSH and Nrf2 pathway contributing to the radioresistance of tumor cells.

radiation exposure. This may be due to the fact that some basal levels of Nrf2 are required for maintaining the cellular oxidative homeostasis. When Nrf2 is knocked down, even under normal circumstances, it will lead to the accumulation of higher levels of ROS and that may affect the cell survival [31].

In conclusion, in this study, we have demonstrated the role of Nrf2 and its dependent genes in radioresistance of prostate tumor cells through management of intracellular ROS and GSH levels (Fig. 8). As the radioresistance is the serious impediment in radiotherapy, Nrf2 inhibition can be used as a target to enhance the ionizing radiation induced tumor killing.

Conflict of interest

The authors declare no conflicts of interest.

Acknowledgements

Authors would like to thank Mr. B.A. Naidu for technical assistance and Ms. Jisha Menon for help in flow cytometry studies. Authors would also like to thank Dr. Geetanjali Sachdeva from the National Institute for Research in Reproductive Health, for providing us both PC3 and DU145 cell lines and the Department of Atomic Energy, India, for funding this study.

References

[1] L. Peters, M. McKay, Predictive assays: will they ever have a role in the clinic? Int. J. Radiat. Oncol. Biol. Phys. 49 (2001) 501–504.
[2] D. Gius, Redox-sensitive signaling factors and antioxidants: how tumor cells respond to ionizing radiation, J. Nutr. 134 (2004) 3213S–3214S.
[3] H.C. Lee, D.W. Kim, K.Y. Jung, I.C. Park, M.J. Park, M.S. Kim, S.H. Woo, C.H. Rhee, H. Yoo, S.H. Lee, S.I. Hong, Increased expression of antioxidant enzymes in radioresistant variant from U251 human glioblastoma cell line, Int. J. Mol. Med. 13 (2004) 883–887.
[4] T. Nguyen, P. Nioi, C.B. Pickett, The Nrf2–antioxidant response element signaling pathway and its activation by oxidative stress, J. Biol. Chem. 284 (2009) 13291–13295.
[5] N. Wakabayashi, S.L. Slocum, J.J. Skoko, S. Shin, T.W. Kensler, When NRF2 talks, who's listening? Antioxid. Redox Signal. 13 (2010) 1649–1663.
[6] P. Zhang, A. Singh, S. Yegnasubramanian, D. Esopi, P. Kombairaju, M. Bodas, H. Wu, S.G. Bova, S. Biswal, Loss of Kelch-like ECH-associated protein 1 function in prostate cancer cells causes chemoresistance and radioresistance and promotes tumor growth, Mol. Cancer Ther. 9 (2010) 336–346.
[7] A. Singh, M. Bodas, N. Wakabayashi, F. Bunz, S. Biswal, Gain of Nrf2 function in non-small-cell lung cancer cells confers radioresistance, Antioxid. Redox Signal. 13 (2010) 1627–1637.
[8] T. Shibata, A. Kokubu, S. Saito, M. Narisawa-Saito, H. Sasaki, K. Aoyagi, Y. Yoshimatsu, Y. Tachimori, R. Kushima, T. Kiyono, M. Yamamoto, NRF2 mutation confers malignant potential and resistance to chemoradiation therapy in advanced esophageal squamous cancer, Neoplasia 13 (2011) 864–873.
[9] M.J. Szostak, N. Kyprianou, Radiation-induced apoptosis: predictive and therapeutic significance in radiotherapy of prostate cancer (Review), Oncol. Rep. 7 (2000) 699–706.
[10] P. Pettazzoni, E. Ciamporcero, C. Medana, S. Pizzimenti, F. Dal Bello, V.G. Minero, C. Toaldo, R. Minelli, K. Uchida, M.U. Dianzani, R. Pili, G. Barrera, Nuclear factor erythroid 2-related factor-2 activity controls 4-hydroxynonenal metabolism and activity in prostate cancer cells, Free Radic. Biol. Med. 51 (2011) 1610–1618.
[11] K.J. Niermann, L. Moretti, N.J. Giacalone, Y. Sun, S.M. Schleicher, P. Kopsombut, L.R. Mitchell, K.W. Kim, B. Lu, Enhanced radiosensitivity of androgen-resistant prostate cancer: AZD1152-mediated Aurora kinase B inhibition, Radiat. Res. 175 (2011) 444–451.
[12] M. Zhang, M. Siedow, G. Saia, A. Chakravarti, Inhibition of p21-activated kinase 6 (PAK6) increases radiosensitivity of prostate cancer cells, Prostate 70 (2010) 807–816.
[13] J. Lovey, D. Nie, J. Tovari, I. Kenessey, J. Timar, M. Kandouz, K.V. Honn, Radiosensitivity of human prostate cancer cells can be modulated by inhibition of 12-lipoxygenase, Cancer Lett. 335 (2013) 495–501.
[14] N.A.P. Franken, H.M. Rodermond, J. Stap, J. Haveman, C. van Bree, Clonogenic assay of cells in vitro, Nat. Protoc. 1 (2006) 2315–2319.
[15] S. Jayakumar, H.N. Bhilwade, B.N. Pandey, S.K. Sandur, R.C. Chaubey, The potential value of the neutral comet assay and the expression of genes associated with DNA damage in assessing the radiosensitivity of tumor cells, Mutat. Res. 748 (2012) 52–59.
[16] S.K. Sandur, H. Ichikawa, G. Sethi, K.S. Ahn, B.B. Aggarwal, Plumbagin (5-hydroxy-2-methyl-1,4-naphthoquinone) suppresses NF-kappaB activation and NF-kappaB-regulated gene products through modulation of p65 and IkappaBalpha kinase activation, leading to potentiation of apoptosis induced by cytokine and chemotherapeutic agents, J. Biol. Chem. 281 (2006) 17023–17033.
[17] A. Kunwar, S. Jayakumar, H.N. Bhilwade, P.P. Bag, H. Bhatt, R.C. Chaubey, K.I. Priyadarsini, Protective effects of selenocystine against gamma-radiation-induced genotoxicity in Swiss albino mice, Radiat. Environ. Biophys. 50 (2011) 271–280.
[18] B.N. Pandey, K.P. Mishra, Modification of thymocytes membrane radiooxidative damage and apoptosis by eugenol, J. Environ. Pathol. Toxicol. Oncol. 23 (2004) 117–122.
[19] B. Kumar, A. Kumar, S. Ghosh, B.N. Pandey, K.P. Mishra, B. Hazra, Diospyrin derivative, an anticancer quinonoid, regulates apoptosis at endoplasmic reticulum as well as mitochondria by modulating cytosolic calcium in human breast carcinoma cells, Biochem. Biophys. Res. Commun. 417 (2012) 903–909.
[20] I. Rahman, A. Kode, S.K. Biswas, Assay for quantitative determination of glutathione and glutathione disulfide levels using enzymatic recycling method, Nat. Protoc. 1 (2006) 3159–3165.
[21] S. Singh, D. Chitkara, R. Mehrazin, S.W. Behrman, R.W. Wake, R.I. Mahato, Chemoresistance in prostate cancer cells is regulated by miRNAs and Hedgehog pathway, PLoS One 7 (2012) e40021.
[22] J.T. Lee Jr., L.S. Steelman, J.A. McCubrey, Phosphatidylinositol 3′-kinase activation leads to multidrug resistance protein-1 expression and subsequent chemoresistance in advanced prostate cancer cells, Cancer Res. 64 (2004) 8397–8404.
[23] B.E. Lehnert, R. Iyer, Exposure to low-level chemicals and ionizing radiation: reactive oxygen species and cellular pathways, Hum. Exp. Toxicol. 21 (2002) 65–69.
[24] J. Sun, Y. Chen, M. Li, Z. Ge, Role of antioxidant enzymes on ionizing radiation resistance, Free Radic. Biol. Med. 24 (1998) 586–593.

[25] E.A. Bump, J.M. Brown, Role of glutathione in the radiation response of mammalian cells in vitro and in vivo, Pharmacol. Ther. 47 (1990) 117–136.
[26] N. Mirkovic, D.W. Voehringer, M.D. Story, D.J. McConkey, T.J. McDonnell, R.E. Meyn, Resistance to radiation-induced apoptosis in Bcl-2-expressing cells is reversed by depleting cellular thiols, Oncogene 15 (1997) 1461–1470.
[27] R. Brigelius-Flohe, L. Flohe, Basic principles and emerging concepts in the redox control of transcription factors, Antioxid. Redox Signal. 15 (2011) 2335–2381.
[28] M. Tsukimoto, N. Tamaishi, T. Homma, S. Kojima, Low-dose gamma-ray irradiation induces translocation of Nrf2 into nuclear in mouse macrophage RAW264.7 cells, J. Radiat. Res. 51 (2010) 349–353.
[29] T.W. Kensler, N. Wakabayashi, S. Biswal, Cell survival responses to environmental stresses via the Keap1–Nrf2–ARE pathway, Annu. Rev. Pharmacol. Toxicol. 47 (2007) 89–116.
[30] M. Tanito, M.P. Agbaga, R.E. Anderson, Upregulation of thioredoxin system via Nrf2–antioxidant responsive element pathway in adaptive-retinal neuroprotection in vivo and in vitro, Free Radic. Biol. Med. 42 (2007) 1838–1850.
[31] J.T. McDonald, K. Kim, A.J. Norris, E. Vlashi, T.M. Phillips, C. Lagadec, L. Della Donna, J. Ratikan, H. Szelag, L. Hlatky, W.H. McBride, Ionizing radiation activates the Nrf2 antioxidant response, Cancer Res. 70 (2010) 8886–8895.